

# The Importance of the Montreal Protocol in Mitigating the Potential Intensity of Tropical Cyclones

LORENZO M. POLVANI

*Department of Applied Physics and Applied Mathematics, and Department of Earth and Environmental Sciences,  
Lamont-Doherty Earth Observatory, Columbia University, New York, New York*

SUZANA J. CAMARGO

*Lamont-Doherty Earth Observatory, Columbia University, Palisades, New York*

ROLANDO R. GARCIA

*National Center for Atmospheric Research, Boulder, Colorado*

(Manuscript received 30 March 2015, in final form 19 December 2015)

## ABSTRACT

The impact of the Montreal Protocol on the potential intensity of tropical cyclones over the next 50 years is investigated with the Whole Atmosphere Community Climate Model (WACCM), a state-of-the-art, stratosphere-resolving atmospheric model, coupled to land, ocean, and sea ice components, with interactive stratospheric chemistry. An ensemble of WACCM runs from 2006 to 2065 forced with a standard future scenario is compared to a second ensemble in which ozone-depleting substances (ODS) are not regulated (the so-called World Avoided). It is found that by the year 2065, changes in the potential intensity of tropical cyclones in the World Avoided are nearly 3 times as large as for the standard scenario. The Montreal Protocol thus provides a strong mitigation of the adverse effects of intensifying tropical cyclones.

The relative importance of warmer sea surface temperatures (ozone-depleting substances are important greenhouse gases) and cooler lower-stratospheric temperatures (accompanying the massive destruction of the ozone layer) is carefully examined. It is found that the former are largely responsible for the increase in potential intensity in the World Avoided, whereas temperatures above the 70-hPa level—which plunge by nearly 15 K in 2065 in the World Avoided—have no discernible effect on potential intensity. This finding suggests that the modest (compared to the World Avoided) tropical ozone depletion of recent decades has not been a major player in determining the intensity of tropical cyclones, and neither will ozone recovery be in the coming half century.

## 1. Introduction

The discovery of the ozone hole (Farman et al. 1985) and of the key role of halogenated ozone-depleting substances [ODS; see Solomon (1999) for a review of the concepts and history] led to the negotiation and ratification of the Montreal Protocol On Substances that Deplete the Ozone Layer in the late 1980s. The driving force behind the rapid implementation of the Montreal Protocol was the fear that the destruction of the ozone

layer would cause severe adverse effects for public health (e.g., skin cancer) and the environment (e.g., damage to crops); recall that the ozone layer absorbs harmful solar UVB radiation and thus prevents it from reaching Earth's surface.

What was not appreciated at the time of signing, and has become apparent only in the last decade, is that the Montreal Protocol has turned out to be a powerful climate mitigation treaty as well. In terms of radiative forcing alone, for instance, the greenhouse effect associated with the reduction in ODS has resulted in an abatement of  $0.8\text{--}1.6\text{ W m}^{-2}$  by 2010, a number comparable to the one associated with the forcing from  $\text{CO}_2$  alone since preindustrial times (Velders et al. 2007). Even more important, however, is the impact of ODS on

---

*Corresponding author address:* Lorenzo M. Polvani, S.W. Mudd Room 216, Columbia University, Mail Code 4701, New York, NY 10027.  
E-mail: lmp@columbia.edu

the climate system via the formation of the ozone hole. Ozone depletion has resulted in a dramatic cooling in the lower stratosphere over the South Pole; such a cooling is able to induce a substantial poleward shift of the midlatitude jet, affecting surface temperatures, clouds, and precipitation, at both low and midlatitudes. The jet shift also causes considerable changes in momentum, heat, and salinity fluxes at the ocean surface; hence, the formation of the ozone hole is felt deep in the Southern Ocean, affecting temperature, salinity, and sea ice. Two recent reviews, [Thompson et al. \(2011\)](#) and [Previdi and Polvani \(2014\)](#), detail the profound impacts of the ozone hole over the climate system of the Southern Hemisphere.

An alternative line of inquiry can be pursued to assess the climate impacts of the Montreal Protocol. It consists in asking the following simple question: what would have happened, in the coming decades, if the Montreal Protocol had not been implemented? This line of inquiry is commonly referred to as the “World Avoided” scenario. Most of the literature on the World Avoided ([Prather et al. 1996](#); [Newman et al. 2009](#)) has focused on documenting the global catastrophic collapse of ozone concentrations by the 2060s in the absence of ODS regulations. More recently, however, a few studies have started to examine the surface climate in the World Avoided. Owing to the powerful greenhouse effect of increasing ODS ([Ramanathan 1975](#)), the global mean surface temperature in the World Avoided would increase by 2.5 K by 2070, with clear signatures of polar amplification ([Morgenstern et al. 2008](#); [Garcia et al. 2012](#)). Furthermore, changes in the hydrological cycle in the World Avoided would be twice as large as those currently projected by 2025 ([Wu et al. 2013](#)).

Pursuing this line of inquiry, we here explore yet another unintended consequence of the Montreal Protocol: its role in mitigating the future strengthening of tropical cyclones. We do this by comparing model simulations of the World Avoided, over the period 2006–65, with corresponding simulations over the same period in which ODS are regulated per Montreal Protocol. Beyond documenting an important impact of the Montreal Protocol, understanding how the intensity of tropical cyclones might change in a warming climate is a matter of great scientific interest [see [Knutson et al. \(2010\)](#) for a recent review], especially in view of the major societal impacts of these powerful storms ([Mendelsohn et al. 2012](#); [Peduzzi et al. 2012](#)).

A common way of addressing this issue is to employ a theoretical estimate known as the potential intensity (PI) of tropical cyclones. Originally proposed by [Emanuel \(1995\)](#), and later refined by [Bister and](#)

[Emanuel \(1998\)](#), this quantity can be computed from reanalyses or model output on relatively coarse grids (i.e., without the need to computationally resolve individual tropical cyclones). The PI simply estimates the maximum possible wind speed a tropical cyclone might be able to attain as a function of a few simple parameters: the sea surface temperature  $T_s$ , the convective available potential energy (CAPE) at the radius of maximum winds, and the outflow temperature  $T_o$  (i.e., the temperature where a rising parcel is at the level of neutral buoyancy, typically around tropopause). There is evidence suggesting a close relationship between PI and actual tropical cyclone intensity ([Wing et al. 2007](#); [Kossin and Camargo 2009](#)).

The World Avoided scenario, which might be considered highly unrealistic at first glance, actually offers a very interesting test bed for understating how the intensity of tropical cyclone might change in a warming climate. On one hand, the greenhouse effect of ODS yields much warmer  $T_s$  in the World Avoided, with expected impacts on PI similar to those of increasing  $\text{CO}_2$  (see, e.g., [Vecchi and Soden 2007](#); [Camargo 2013](#)). On the other hand, the global and severe depletion of the ozone layer in the World Avoided results in a very significant cooling in the tropical lower stratosphere (almost 15 K by 2065), and this could also have a large impact on PI by altering the outflow temperature  $T_o$ .

In fact, the degree to which lower-stratospheric tropical cooling is able to affect PI is a matter of much recent debate. [Emanuel et al. \(2013\)](#) have presented observational evidence that temperatures at the 70-hPa level, which show a cooling of about  $1 \text{ K decade}^{-1}$  over the 1980–2010 period in some reanalysis datasets, have contributed to the observed increase in PI over the North Atlantic over the same period. The importance of lower-stratospheric temperature for PI is further corroborated by two idealized studies, using both two-dimensional ([Ramsay 2013](#)) and three-dimensional ([Wang et al. 2014](#)) idealized hurricane models; these clearly show that colder tropopause temperatures result in considerably stronger tropical cyclones.

However, the importance of temperature trend at levels above 100 hPa in calculations of PI has recently been questioned by [Vecchi et al. \(2013\)](#). In that study, using a high-resolution global climate model, the authors showed that temperature trends at levels of 70 hPa and above have no impact on PI, at least over the last three decades. In addition, [Wing et al. \(2015\)](#) have shown that differences between outflow and sea surface temperatures—which capture the thermodynamic efficiency of the system—seem to have played a very minor role, at best, in determining PI multidecadal trends since

1979 [see Figs. 2a,b of [Wing et al. \(2015\)](#)]. Nonetheless one might still argue that, while lower-stratospheric temperature trends have not been large enough in the last several decades to have a noticeable impact felt at present, they might perhaps matter in the future as the stratosphere cools more robustly with continually increasing concentrations of CO<sub>2</sub>.

The World Avoided scenario, in which the massive destruction of the ozone layer causes very large trends in the lower stratosphere, therefore offers an excellent circumstance to evaluate whether lower-stratospheric temperatures are able to impact the potential intensity of tropical cyclones. To explore this possible impact we proceed as follows. In [section 3](#) we describe the World Avoided simulations we have performed, in terms of both the specified forcing and the climate response. The dramatic increase in PI in the World Avoided is then documented in [section 4](#), in which we contrast the World Avoided trends with those of widely used standard future scenarios. In [section 5](#) we carefully assess, following the methodology of [Vecchi et al. \(2013\)](#), how temperature trends in various atmospheric layers are able to influence PI; we find that PI is largely insensitive to trends at 70 hPa and above, even when these trends are very large (as in the case of the World Avoided). [Section 6](#) closes the paper with a discussion of outstanding issues.

## 2. Methods

### a. The model

To compute the climate of the World Avoided scenario, we here employ one of the climate models available within the Community Earth System Model, version 1 (CESM1; [Hurrell et al. 2013](#)); specifically, we use the Whole Atmosphere Community Climate Model (WACCM). This model participated in phase 5 of the Coupled Model Intercomparison Project (CMIP5), and submitted both historical and representative concentration pathway (RCP) integrations. The version of WACCM used here has been fully documented by [Marsh et al. \(2013\)](#), to which the reader is referred for all details about the model configuration. We here only review a few salient facts, to familiarize the reader with WACCM.

In a nutshell, WACCM is a stratosphere- and mesosphere-resolving atmospheric model. The vertical domain, which extends to 140 km in altitude, is discretized by 66 hybrid levels (which become isobaric above 100 hPa). The horizontal resolution is  $1.9^{\circ} \times 2.5^{\circ}$  in latitude and longitude, respectively. This atmospheric model is coupled to ocean, land, and sea ice components, which are identical, in nearly every respect, to those of the

“low-top” Community Climate System Model, version 4 (CCSM4; [Gent et al. 2011](#)). The key additional feature of WACCM is that it includes a fully interactive middle atmosphere chemistry package (59 species, 217 gas-phase chemical reactions, and 17 heterogeneous reactions on three aerosol types) so that stratospheric ozone is computed self-consistently with the temperature and circulation of the middle atmosphere.

### b. The model integrations

The first set of WACCM integrations examined here are canonical RCP4.5 runs, per the CMIP5 protocol ([Taylor et al. 2012](#)). In these, the non-ODS greenhouse gas concentrations (CO<sub>2</sub>, CH<sub>4</sub>, and N<sub>2</sub>O) follow the  $4.5 \text{ W m}^{-2}$  “stabilization” pathway ([Van Vuuren et al. 2011](#); [Meinshausen et al. 2011b](#)); surface concentrations of ODS follow scenario A1 of the [World Meteorological Organization \(2007\)](#), resulting from the implementation of the Montreal Protocol and its amendments, with minor modifications ([Meinshausen et al. 2011a](#)). An ensemble of three such WACCM integrations, over the period 2006 to 2065, are available to us; we refer to these as the RCP4.5 runs.

The second set of three integrations are the World Avoided runs, labeled RCP4.5WA. As the name suggests, these are identical to the RCP4.5 runs in every respect, except for the surface concentrations of ODS. Following [Garcia et al. \(2012, hereafter GKM12\)](#), ODS are here chosen to increase at a constant rate of  $3.5\% \text{ yr}^{-1}$ , starting from 1985. In fact, our World Avoided runs are very similar to the one analyzed in detail in [GKM12](#); we here use the same model configuration and forcings. The only difference with [GKM12](#) is that, to acquire some sense of internal variability, we here analyze an ensemble of three such runs, instead of a single one.

Third, in addition to these two ensembles whose direct comparison allows us to quantify the effects of the Montreal Protocol, we also make use of two additional three-member ensembles of WACCM runs. One is a set of WACCM historical integrations from 1955 to 2005, with all forcings per the CMIP5 specifications; these runs were carefully analyzed in [Marsh et al. \(2013\)](#), and we here simply use them to compute difference between the past and the present. The other is a set of WACCM runs with the CMIP5 RCP8.5 scenario; this allows us to compare the World Avoided conditions with those of a climate with larger greenhouse gas concentrations. For obvious reasons, we will refer to these two additional ensembles as historical and RCP8.5.

As WACCM is a relatively new climate model, we also compare our WACCM runs with the low-top companion CESM model (CCSM4; [Gent et al. 2011](#));

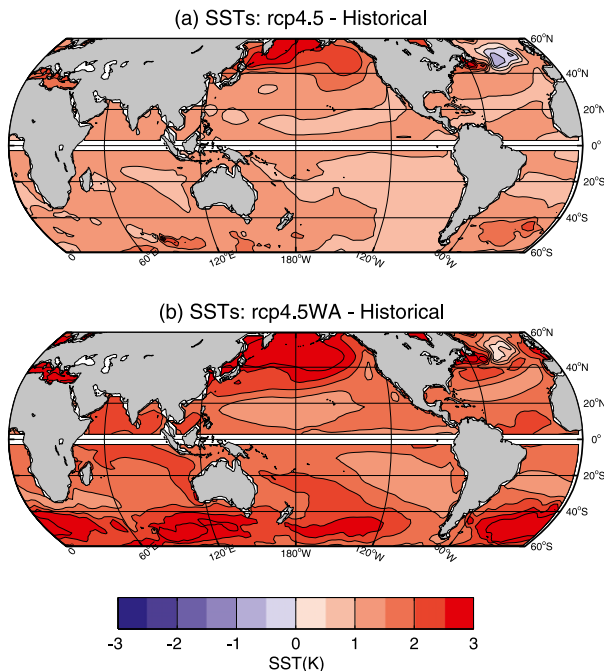


FIG. 1. Ensemble mean SST differences in the future scenarios (2056–65) to the historical values (1980–89): (a) RCP4.5 runs and (b) RCP4.5WA runs. In both panels, the average for ASO is shown for the Northern Hemisphere and for JFM for the Southern Hemisphere. All panels are Robinson projections, extending from 60°S to 60°N.

six-member ensembles are available for the historical simulations, as well as the RCP4.5 and RCP8.5. Last, to put our results in an even broader context, we contrast WACCM potential intensity with the multimodel mean (MMM) of 25 CMIP5 models (the CMIP5 models used here are listed in the appendix). For the interested reader, we note that the PI of each individual CMIP5 model used in this study has already been documented in either Camargo et al. (2013), for 14 models, or Ting et al. (2015), for 25 models.

### 3. Temperatures in the World Avoided

Because ODS are powerful greenhouse gases, we start by recalling how surface temperatures rise considerably more in the World Avoided than in the corresponding standard CMIP5 scenario. This is not surprising given that, as noted in GKM12, the radiative forcing in the RCP4.5WA runs is almost double that of the RCP4.5 runs by 2065. As we are here primarily interested in tropical cyclones, we illustrate this by showing the sea surface temperature (SST) changes.

In Fig. 1, each panel shows the ensemble mean difference between the last decade of the future integrations (2056–65) and a decade in the recent past (we

use 1980–89, just prior to the signing of the Montreal Protocol). Since we plan to discuss tropical cyclones, we do not just show differences in the annual mean; north of the equator we take the average of the three months August–October (ASO) and south of the equator the average of January–March (JFM), corresponding to the peak tropical cyclone season in each hemisphere—hence the white area around the equator (where no tropical cyclones form), to alert the reader of the different seasons to the north and to the south. This same plotting scheme applies to all latitude–longitude figures in this paper.

It is easy to see from Fig. 1 that by the 2060s the SSTs are considerably warmer in the World Avoided (Fig. 1b) than in the corresponding future scenario runs (Fig. 1a). More precisely, the warming is 1.7 times larger in the Northern Hemisphere (NH) and 1.9 times larger in the Southern Hemisphere (SH); this is roughly in line with the radiative forcing difference. Similar differences in global mean atmospheric surface temperature were reported in GKM12 (see their Fig. 11).

More interesting, perhaps, is what occurs in the lower stratosphere in the World Avoided. Start by recalling that, in such a scenario, the unregulated emission of halogenated ODS results in a massive destruction of the ozone layer. Following Newman et al. (2009), we quantify the ODS burden using the so-called equivalent effective chlorine (EECL); this is a linear combination of the mixing ratios of ODS (i.e., CFCs, HCFCs, CCl<sub>4</sub>, halons, and a few others; see Table 1 of GKM12 for details) weighted by their ozone-depleting efficiency. As shown in Fig. 2a, EECL declines steadily in the twenty-first century as a consequence of the Montreal Protocol (blue curve) but grows dramatically in the World Avoided scenario (red curve). As a consequence, in that scenario the ozone layer collapses after 2040, as seen in Fig. 2b; roughly 3/4 of the tropical ozone at 50 hPa is destroyed by 2065 in the RCP4.5WA integrations.

The direct radiative effect of such massive ozone depletion is a dramatic cooling of the lower stratosphere, as solar UV absorption by ozone is greatly reduced at those levels. Tropical temperature profiles for the historical pre-Montreal Protocol period (1980–89, black) and for the last decade of the scenario runs (2056–65, RCP4.5 in blue and RCP4.5WA in red) are plotted in Fig. 3; Fig. 3a shows the ASO months (relevant for NH tropical cyclones), and Fig. 3b shows JFM (for the SH). Note that at 50 hPa the World Avoided cooling is over 15 K by the end of the runs, compared to only a few degrees for the standard scenario. Even at 70 hPa, the World Avoided cooling is substantially

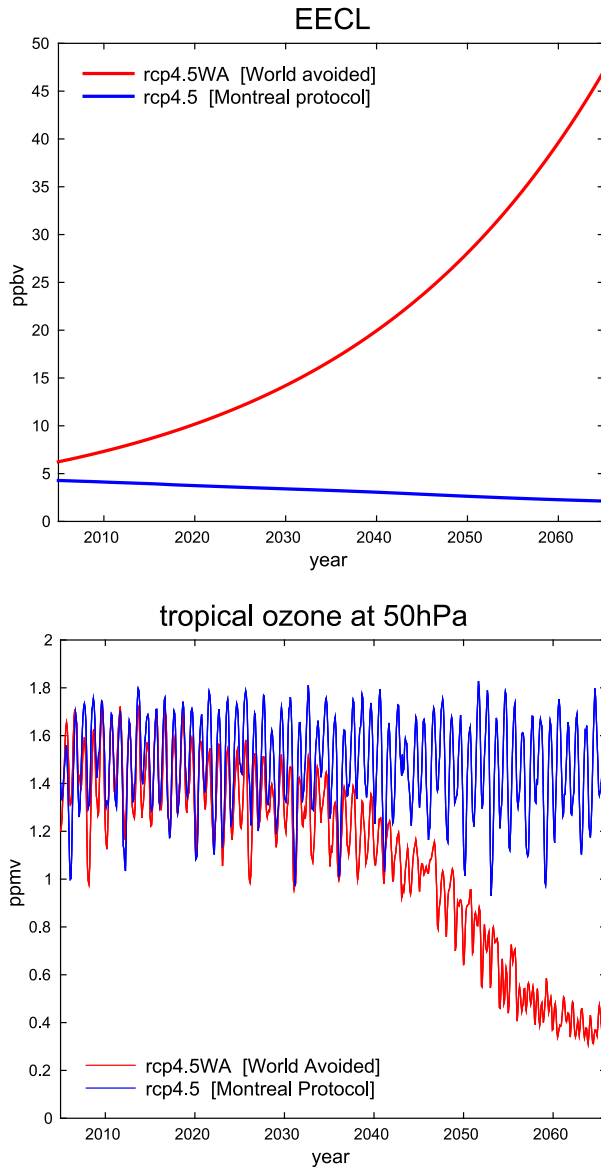


FIG. 2. (a) Surface concentrations of EECL (see text for definition), in ppbv. (b) Ensemble mean, monthly WACCM ozone concentrations at 50 hPa, averaged from 30°N to 30°S, in ppmv. Blue curves denote RCP4.5 runs, and red curves denote RCP4.5WA runs.

larger. One might suppose that such dramatic cooling could affect the intensity of tropical cyclones, as recently suggested (Emanuel 2010; Emanuel et al. 2013); we now turn our attention to this question.

#### 4. Potential intensity in the World Avoided

A widely used tool to ascertain how tropical cyclone strength may change in a changing climate is the so-called potential intensity  $V_{pot}$ , a theoretical estimate of

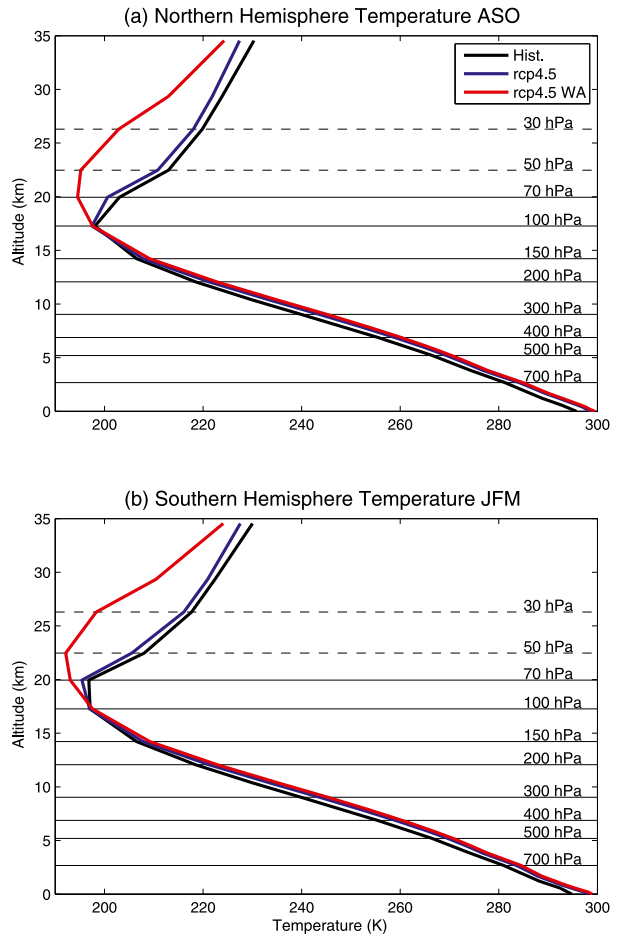


FIG. 3. Tropical temperature profiles, 30°S to 30°N, for the (a) Northern and (b) Southern Hemisphere, in ASO and JFM, respectively. Each curve shows the ensemble mean of three WACCM runs. Black curves denote the 1980–99 average of the historical runs, blue curves denote the 2056–65 average of the RCP4.5 runs, and red curves denote the 2056–65 average of the RCP4.5WA runs. Horizontal lines denote the levels used in the computation of potential intensity (levels below 700 hPa are not shown). The dashed levels (30 and 50 hPa) are here used in the computation of PI\* (see text) but have been traditionally excluded from the computation of PI.

the upper bound on the azimuthal wind speed that may be reached by tropical cyclones given environmental conditions (Emanuel 1988). We here closely follow the methodology of Bister and Emanuel (2002), who define it as follows:

$$V_{pot}^2 = \frac{C_k}{C_D} \frac{T_s}{T_o} [CAPE^* - CAPE]_{RMW}. \quad (1)$$

In this expression,  $C_k$  and  $C_D$  are the heat exchange and drag coefficients,  $T_s$  is the SST and  $T_o$  the outflow temperature, CAPE is the convective available potential energy, and CAPE\* is the convective available potential

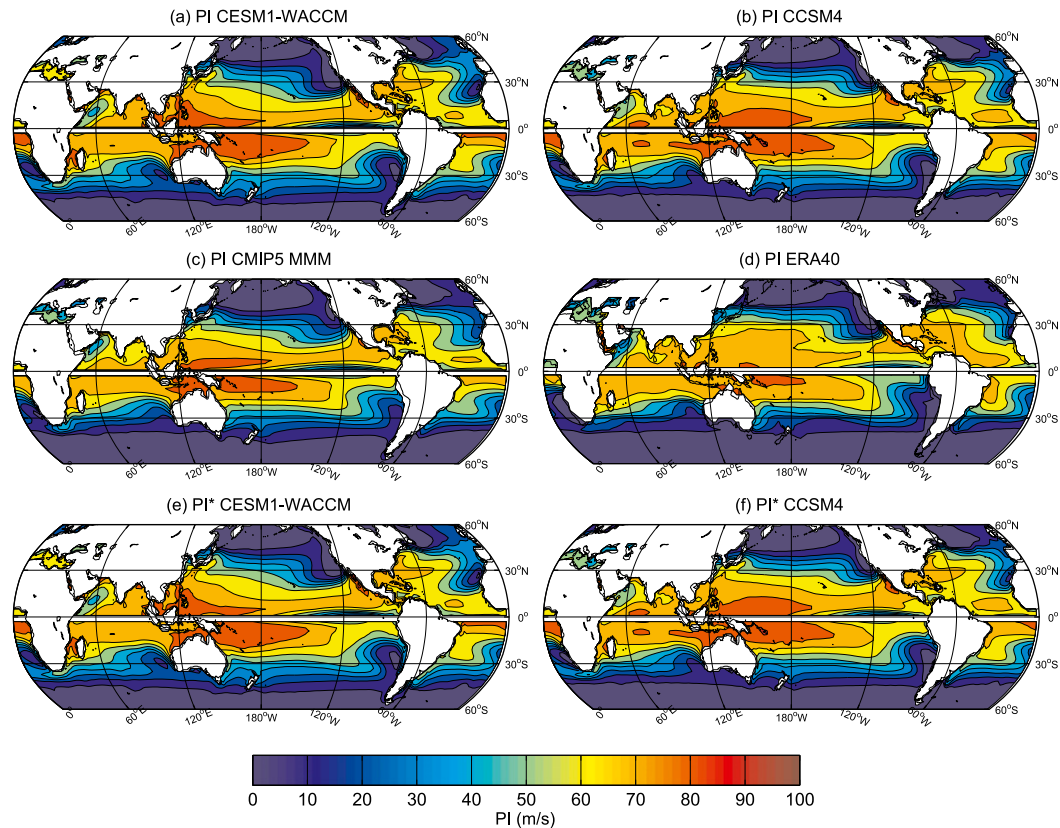


FIG. 4. Climatology of potential intensity for the period 1971–2000. PI, computed with the top level at 70 hPa, is shown for (a) WACCM (three-member mean), (b) CCSM4 (six-member mean, from CMIP5), (c) CMIP5 MMM (25 models), and (d) ERA-40. PI\*, with top level at 30 hPa, is shown for (e) WACCM (three-member mean) and (f) CCSM4 (six-member mean). In all panels, ASO months are shown for the Northern Hemisphere and JFM for the Southern Hemisphere.

energy of a saturated air parcel, both computed at the radius of maximum wind (RMW).

It is important to stress that whereas  $T_s$  is immediately available from model output, the values of  $T_o$ , CAPE, and CAPE\* need to be computed from temperature and specific humidity profiles and depend very sensitively on a number of thermodynamic assumptions. In this study we have used a Matlab code [available at <ftp://texmex.mit.edu/pub/emanuel/TCMAX>; more details can be found in Bister and Emanuel (2002) and also in the appendix of Camargo et al. (2007)]. For the record, in this paper we compute PI with dissipative heating switched on and with the parcel ascent based on a reversible adiabat. We also note that we have repeated many of the calculations in this section using a pseudoadiabat for parcel ascent, and the key results presented below here are totally insensitive to the choice of adiabat.

The PI definition in Eq. (1) has been extensively used as a proxy for estimating actual tropical cyclone intensity from low-resolution reanalyses and model output (Camargo

et al. 2013; Ting et al. 2015) because the PI tracks the actual intensity well on interannual and longer time scales (Wing et al. 2007; Kossin and Camargo 2009).

Armed with Eq. (1), we start by validating WACCM, since that model has not previously been used to study PI. The WACCM climate over the historical period has been analyzed by Marsh et al. (2013) and found to be very close to that of CCSM4. For PI, the WACCM values over the period 1971–2000 are shown in Fig. 4a; they are slightly weaker in amplitude to those in CCSM4 (Fig. 4b) but compare favorably to the CMIP5 multimodel mean (25 models) as well as to the PI computed from ERA-40<sup>1</sup> (Figs. 4c and 4d, respectively; Uppala et al. 2005). From this figure, we conclude that WACCM is an adequate model for studying tropical cyclone PI.

<sup>1</sup> We note that the PI values shown in Fig. 4c are simply reproduced from Camargo (2013), who used a slightly older PI code than the one used here.

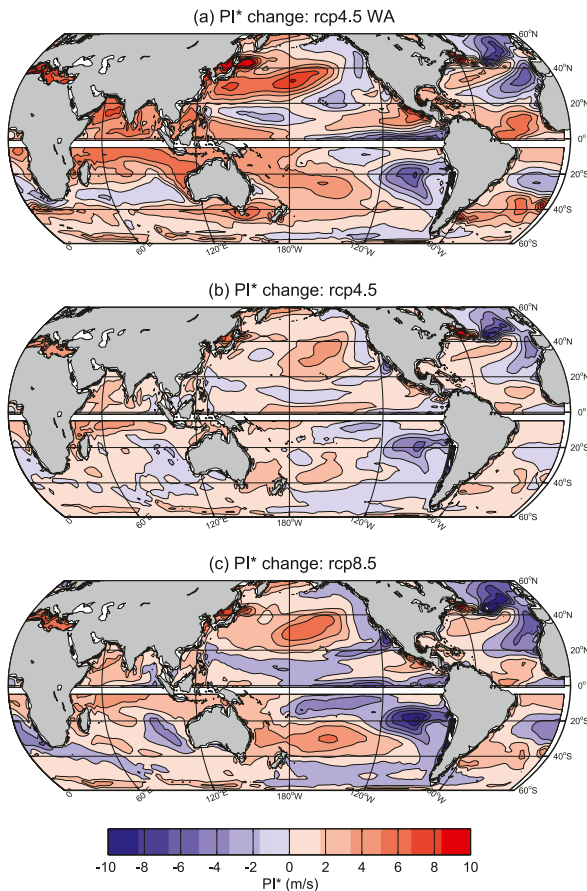


FIG. 5. Differences in  $PI^*$  between the decade 2056–65 and the decade 1980–89. Each plot is the ensemble mean of three WACCM runs. (a) RCP4.5WA, (b) RCP4.5, and (c) RCP8.5. In all panels, ASO months are shown for the Northern Hemisphere and JFM for the Southern Hemisphere.

For historical reasons, the PI computation until recently has been truncated at the 70-hPa level. While not explicitly stated in most papers, this 70-hPa cap was actually present in the widely used code (provided at the URL noted above). A quick perusal of Fig. 3 obviously suggests that, for the stratospheric cooling present in the World Avoided, the bulk of the signal is above 70 hPa. Needless to say, one would want to take this into account. The same may apply, to a lesser degree, to the stratospheric cooling associated with increasing levels  $CO_2$ ; recall that the maximum cooling from greenhouse gases typically occurs at 1 hPa [see, for instance, Fig. 5 of Shine et al. (2003)].

Hence, to properly evaluate the possible sensitivity of tropical cyclone intensity to cooling in the lower stratosphere, we here define a slightly modified version of potential intensity, which we denote  $PI^*$ ; it is identical to PI in every respect but includes data at the 50- and 30-hPa levels, in addition to the levels below that (all levels above

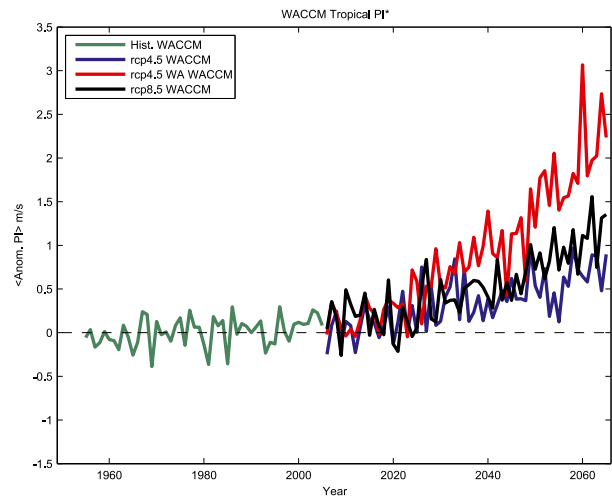


FIG. 6. Tropical ( $30^{\circ}S$  to  $30^{\circ}N$ ), ensemble and annual mean time series of anomalous  $PI^*$ , computed as difference from the 1980–89 mean of the historical runs. Colors indicate different scenarios, as shown in the legend. Each curve is the mean of three WACCM runs.

700 hPa are explicitly shown in Fig. 3). One might wonder whether  $PI^*$  differs in any significant way from PI. It does not, as one can see in Fig. 4e; for WACCM,  $PI^*$  is indistinguishable from PI. The same holds for CCSM4 (cf. Figs. 4f and 4b). The reason for this is simple; as will be shown below, outflow temperatures are typically below 100 hPa, so that the additional levels at 50 and 30 hPa make little difference. Nonetheless, we include them here to allow for the possibility that temperature changes at those high levels might be able to affect potential intensity, which is not immediately obvious a priori.

Having validated WACCM, we now address the central question in this study: what changes in potential intensity might one expect in the World Avoided? The answer is given in Fig. 5a, which shows the ensemble mean change in  $PI^*$  between a pre-Montreal Protocol decade in the historical period (1980–89) and the last decade of the World Avoided integrations (2056–65). Over most regions of interest there is a clear intensification of PI in the World Avoided. More interesting is the contrast with the change in  $PI^*$ , over the same period, for the standard future scenario (the RCP4.5 runs), shown in Fig. 5b; the intensification is much larger in the World Avoided. We also present the change in  $PI^*$  for the RCP8.5 runs, shown in Fig. 5c; again, the  $PI^*$  intensification is noticeably weaker than in the World Avoided case.

To more directly contrast the World Avoided with the other scenarios, in Fig. 6 we plot the time series of annual mean  $PI^*$  anomalies, averaged from  $30^{\circ}S$  to  $30^{\circ}N$ . These anomalies are computed with respect to the 1980–89 mean, and each colored curve is the ensemble mean of three WACCM runs. For both the RCP4.5 (blue) and

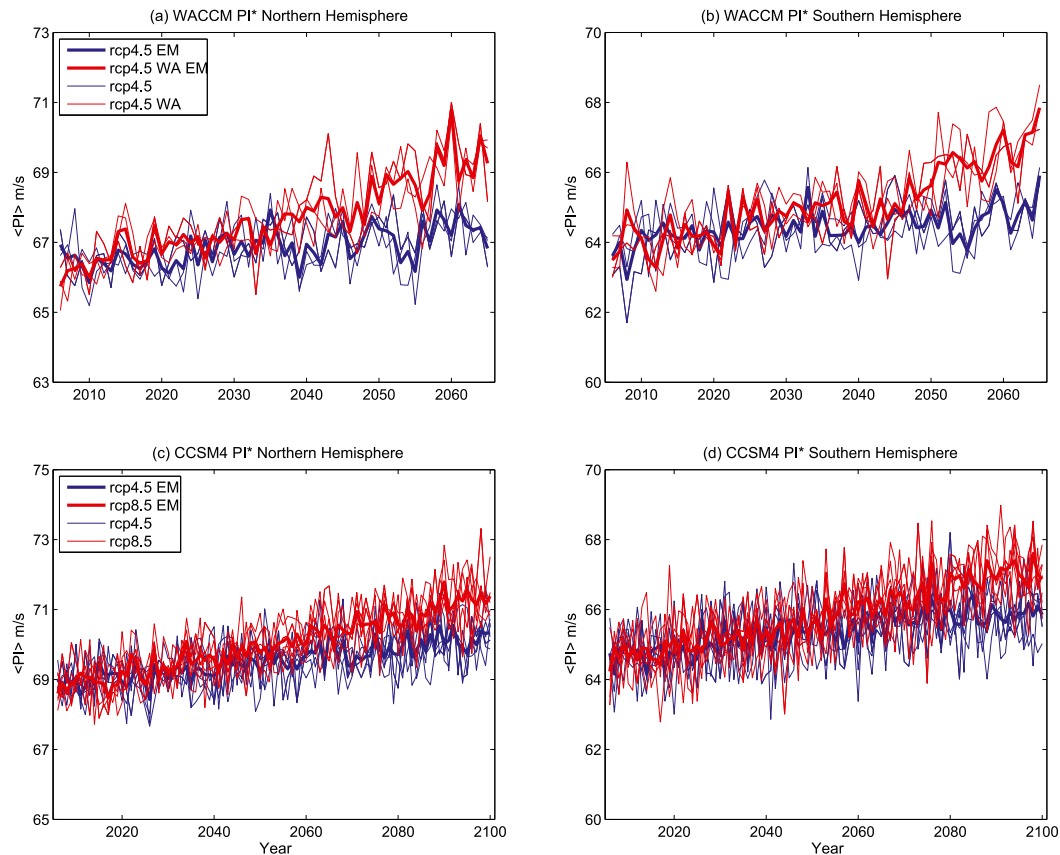


FIG. 7. (top) Time evolution of  $PI^*$  from WACCM for the (a) Northern Hemisphere (ASO) and (b) Southern Hemisphere (JFM); thin lines show individual runs, thick line shows the ensemble mean of three runs, blue curves denote RCP4.5, and red curves denote RCP4.5WA. (bottom) As in (top), but for two six-member ensemble CCSM4 runs; blue curves denote RCP4.5, and red curves denote RCP8.5 for the (c) Northern Hemisphere (ASO) and (d) Southern Hemisphere (JFM).

RCP8.5 (black) scenarios one can see  $PI^*$  increasing well above the historical (green) values; however, for the RCP4.5WA runs (red) the increase is nearly 3 times larger than the one in the RCPs. Hence, the Montreal Protocol has resulted in a very substantial mitigation of tropical cyclone potential intensity in the coming half century.

One might wonder about the statistical significance of our results. Rather than constructing complex statistical tests, we illustrate the robustness of our results by plotting the individual WACCM ensemble members, together with the ensemble mean. This is done in Figs. 7a,b, where we also illustrate the interhemispheric differences in  $PI^*$  trends, plotting the NH in Fig. 7a and the SH in Fig. 7b, for the appropriate seasons. In either panel, it is clear that the spread among ensemble members is considerably smaller than the difference between the RCP4.5WA (red) and RCP4.5 (blue) ensemble mean.

As for interhemispheric differences, they appear to be relatively small. In either hemisphere,  $PI^*$  increases by

nearly  $3 \text{ m s}^{-1}$  in the World Avoided (red) versus  $1 \text{ m s}^{-1}$  in RCP4.5 (blue). This lack of interhemispheric differences is not peculiar to WACCM or to the World Avoided scenario. It can also be seen in Figs. 7c,d, where  $PI^*$  is shown for standard scenarios of CCSM4, the low-top companion model to WACCM. Two different six-member ensembles of runs were performed with CCSM4 for the CMIP5, one for RCP4.5 (blue) and the other for RCP8.5 (red). Small NH/SH differences can be seen in those ensembles. Contrasting Figs. 7a,b and 7c,d, however, we again see that  $PI$  changes in the absence of the Montreal Protocol are considerably larger than any changes between the RCP4.5 and RCP8.5 scenarios.

## 5. Lower-stratospheric temperatures and potential intensity

Having shown that, by 2065, the potential intensity of tropical cyclones increases in the World Avoided nearly 3 times as much as what is projected to occur following the



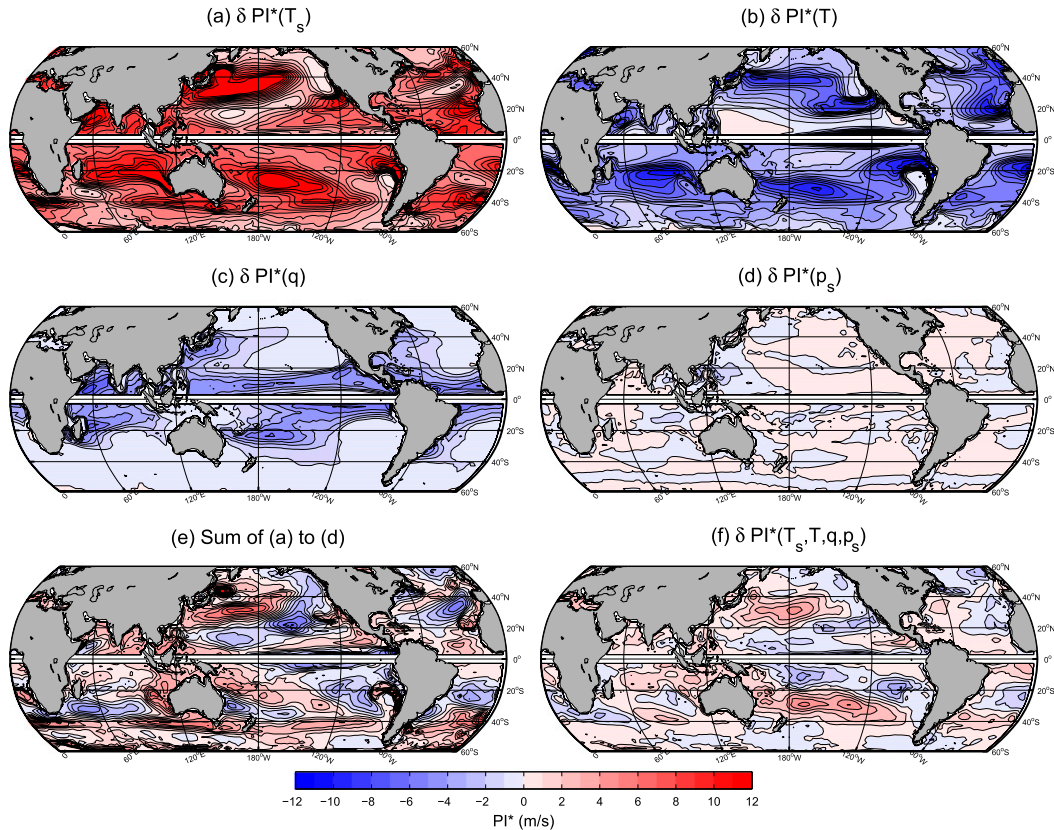


FIG. 8. Maps of  $\delta\text{PI}^*$ , the ensemble mean  $\text{PI}^*$  difference between RCP4.5WA and RCP4.5, averaged over the period 2056–65, due to changes in (a) sea surface temperature  $T_s$ , (b) atmospheric temperature  $T$ , (c) specific humidity  $q$ , and (d) surface pressure  $p_s$  [see Eq. (2)]. (e) The sum of (a)–(d); (f) the actual  $\text{PI}^*$  difference between RCP4.5WA and RCP4.5 [see Eq. (3)].

implementation of the Montreal Protocol, we now wish to dig a little deeper and examine whether the warming SSTs or the cooling lower stratosphere principally controls the changes in PI. This, of course, is of much interest in the context of the broader discussion about the possible impact of lower-stratospheric temperature trends on PI, which we reviewed in the introduction.

A good starting point might be to recall how PI and  $\text{PI}^*$  are actually computed, from model output (or re-analyses). At each latitude, longitude, and time, the input data for the code used in the computation of PI consist of four variables: the SST  $T_s$ , the vertical profiles of atmospheric temperature  $T$  and specific humidity  $q$ , and the surface pressure  $p_s$ . Hence, from an algorithmic point of view, Eq. (1) takes the form  $V_{\text{pot}} = V_{\text{pot}}(T_s, T, q, p_s)$ . So, we start by exploring the role of these four inputs and ask which of them contribute most to the separation of the red and blue curve in Fig. 6 (and Figs. 7a,b). In other words, which of  $T_s$ ,  $T$ ,  $q$ , and  $p_s$  is responsible for the large increase in  $\text{PI}^*$  in the World Avoided compared to the standard RCP4.5 scenario?

The answer can be found in Figs. 8a–d. In each panel, we plot the ensemble mean WACCM difference, over the decade 2056–65, between the  $\text{PI}^*$  for the RCP4.5 runs and the  $\text{PI}^*$  obtained by taking one of the four inputs and substituting the RCP4.5 values with the RCP4.5WA values. In other words, the quantity shown in Fig. 8a, denoted  $\delta\text{PI}^*(T_s)$  for brevity, is

$$\delta\text{PI}^*(T_s) = V_{\text{pot}}(T_s^{\text{WA}}, T, q, p_s) - V_{\text{pot}}(T_s, T, q, p_s), \quad (2)$$

where all inputs are taken from the RCP4.5 runs, except the one with the superscript WA, which is taken from the RCP4.5WA runs. Similarly, in Figs. 8b–d we show  $\delta\text{PI}^*(T)$ ,  $\delta\text{PI}^*(q)$ , and  $\delta\text{PI}^*(p_s)$ , respectively.

Several items in Fig. 8 are worthy of note. First, as one can see from Figs. 8a–d, SSTs and atmospheric temperatures are the key contributors to the difference in  $\text{PI}^*$  between RCP4.5 and RCP4.5WA, with specific humidity and surface pressure playing smaller roles. Second, observe how the changes due to  $T_s$  and  $T$  are nearly everywhere of opposite sign so that differences in the World Avoided actually result from large cancellations. The sum

of Figs. 8a–d is shown in Fig. 8e; because of the complicated cancellations, it is quite difficult to infer the blue/red patterns in that panel by visual inspection of the four individual components.

Third, in Fig. 8f we show the following difference:

$$V_{\text{pot}}(T_s^{\text{WA}}, T^{\text{WA}}, q^{\text{WA}}, p_s^{\text{WA}}) - V_{\text{pot}}(T_s, T, q, p_s), \quad (3)$$

which is identical to the difference between Figs. 5a and 5b. If the computation of PI were a linear operation, Figs. 8e and 8f would be identical. While there are a few similarities between those two panels, one also notes many substantial differences. In fact, close inspection of any one particular region reveals large discrepancies in the actual values. This indicates a considerable amount of nonlinearity in the PI computation, which makes it difficult to determine a priori how the change in any one variable will affect PI at specific locations.

Fourth, and most importantly, let us return to Fig. 8b. Notice that the figure is overwhelmingly blue, indicating that World Avoided changes in atmospheric temperature reduce PI in nearly all regions of the planet. How does one reconcile that with the recent suggestion (Emanuel et al. 2013) that lower-stratospheric cooling might be responsible for the increase in PI in recent decades? Recall that the most dramatic changes in atmospheric temperature in the World Avoided (see Fig. 3) occur above 100 hPa, with cooling in excess of 10 K at 50 and 30 hPa, associated with massive ozone depletion. If the lower-stratospheric temperatures were the key control on PI in the World Avoided, one would naïvely expect to see a lot of red in Fig. 8b, which would indicate large PI increases.

Therefore, one of two things must be happening to explain the uniformly negative  $\delta\text{PI}^*$  in Fig. 8b. Either the impact of the dramatic cooling in the lower stratosphere in the World Avoided is somehow canceled and overwhelmed by the much smaller warming in the troposphere (which would seem unlikely; take a look at Fig. 3 again), or, more simply, the lower-stratospheric cooling just does not have any substantial impact on potential intensity. Which is it?

To answer that question we now explore the impact on PI of temperature changes at different heights in the atmosphere. We follow the methodology of Vecchi et al. (2013) and group atmospheric levels into four regions: the lower troposphere (levels from 350 hPa to the surface), the upper troposphere (the 300-, 250-, and 200-hPa levels), the tropopause transition layer (TTL; 150- and 100-hPa levels), and the lower stratosphere (70-, 50-, and 30-hPa levels). The 70-hPa level is often used as the top of the TTL (see, e.g., Fueglistaler et al. 2009), but we here prefer to follow Vecchi et al. (2013) and lump it together with the 50- and 30-hPa levels, as these are the levels relevant for

ozone depletion. All these levels are marked clearly in Fig. 3.

Before examining their contribution to change in potential intensity, we illustrate in Fig. 9 the actual WACCM temperature changes in each of these four layers, from 2006 and 2065. Below 70 hPa, typical differences between the RCP4.5 and RCP4.5WA runs are of the order of one or two degrees by 2065 and appear to maximize in the upper troposphere (Fig. 9b). Note also that, below 70 hPa, the RCP4.5WA temperatures are warmer than their RCP4.5 counterparts. In sharp contrast, temperatures in the lower stratosphere are much colder for the World Avoided than for RCP4.5, collapsing by almost 15 K in the year 2065 (Fig. 9d).

With this in mind, consider now  $\delta\text{PI}^*$  for each one of the atmospheric layers individually, plotted in Figs. 10a–d. It is abundantly clear that temperature differences at 70 hPa and above have no discernible impact on  $\text{PI}^*$ ; in fact, even the 150- and 100-hPa levels (Fig. 10c) appear to be contributing very little. These facts are visually demonstrated in Figs. 10e,f; Fig. 10e shows the sum of lower- and upper-tropospheric changes alone (Figs. 10a,b), and Fig. 10f shows the sum of all four levels (Figs. 10a–d). Only minuscule differences can be seen between Figs. 10e and 10f, demonstrating the negligible impact of temperature changes above 150 hPa in our WACCM integrations. We also mention, as a side note, that the differences between Figs. 10f and 8b are also minuscule, unlike the differences between Figs. 8e and 8f, suggesting that some inputs to the PI computation may behave more linearly than others.

More importantly, however, one cannot avoid asking, how is it possible that the massive ozone depletion in the World Avoided—and the huge cooling it induces in the lower stratosphere—have virtually no impact on PI? The answer is given in Fig. 11. In Fig. 11a we reproduce Fig. 9d but add the individual ensemble members to bring out the fact that the interensemble differences are much smaller than the difference between the blue (RCP4.5) and red (RCP4.5WA) curves. That is not the case for Fig. 11b, which shows the outflow temperature  $T_o$ , for the same runs, on the same scale. Recall that  $T_o$  is a key ingredient in evaluation of PI [see Eq. (1)]. As one can see from Fig. 11b, the difference in  $T_o$  between the standard RCP4.5 scenario and the World Avoided is less than 1 K by the end of integration. Why is  $T_o$  so little impacted by the massive ozone loss in the World Avoided? As shown in Fig. 11c, the outflow itself is well below the lower-stratospheric levels (70 hPa and above) where the large cooling is found and, as a consequence, lower-stratospheric temperatures have no appreciable effect on PI.

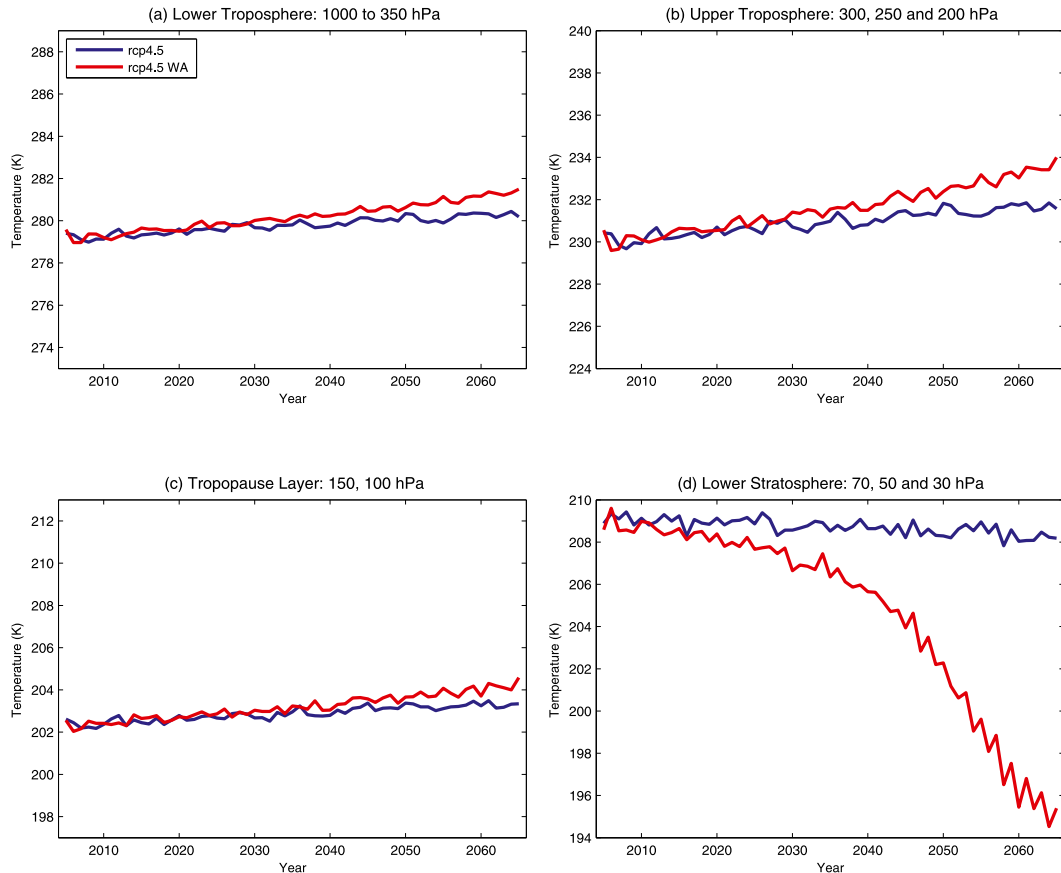


FIG. 9. Ensemble mean, annual mean, tropical ( $30^{\circ}\text{S}$  to  $30^{\circ}\text{N}$ ) temperatures, averaged over (a) the lower troposphere (1000–350 hPa), (b) the troposphere (300, 250, and 200 hPa), (c) the tropical tropopause layer (150 and 100 hPa), and (d) the lower stratosphere (70, 50, and 30 hPa). Red curves are shown for RCP4.5 runs and blue for RCP4.5WA.

## 6. Conclusions

Using a state-of-the-art stratosphere-resolving, atmosphere–ocean coupled model with interactive stratospheric chemistry, and comparing model runs with a standard future scenario to runs of a World Avoided scenario, we have shown that regulation of ODS by the Montreal Protocol will result, in the coming half century, in a substantial mitigation of tropical cyclone potential intensity. We have examined which factors contribute to this mitigation and found that the reduced warming in sea surface temperatures, and not the avoided collapse of the ozone layer, is primarily responsible for the mitigation.

It is now widely appreciated not only that the Montreal Protocol protects the ozone layer (as it was designed to do) but also that it has resulted in substantial mitigation of future changes in surface temperatures (Velders et al. 2007; GKM12) and precipitation (Wu et al. 2013). To the best of our knowledge, the present study is the first to show that the Montreal Protocol is also important in protecting against extreme events, notably tropical cyclones.

One might object that if, in the absence of the Montreal Protocol, much of the ozone layer were to be wiped out by the year 2065, a merely incremental change in hurricane potential intensity would be a relatively minor concern. However, by midcentury, when confronted with an imminent catastrophic collapse of the ozone layer, ODS would likely be immediately banned. In that more plausible alternative scenario (named the “world recovered”), both ozone and lower-stratospheric temperatures recover quickly after ODS emission are banned; in contrast, the ODS-induced warming of the tropospheric and surface temperatures lingers for many decades (see GKM12 for details). That fact, combined with the key finding of this paper—that it is precisely those temperatures that largely control potential intensity—renders the mitigation produced by the Montreal Protocol more practically relevant.

Beyond the Montreal Protocol and the World Avoided scenario, our results have a direct bearing on the current debate (Emanuel et al. 2013; Vecchi et al. 2013) regarding the recent increases in tropical cyclone potential

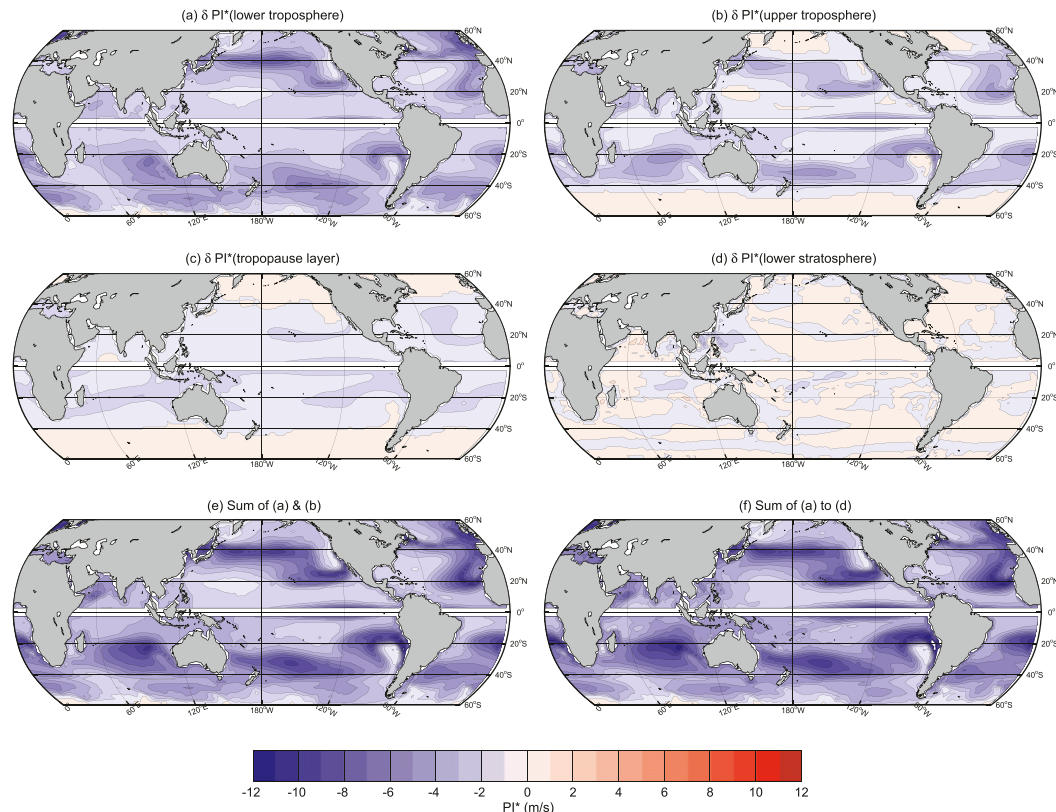


FIG. 10. Ensemble mean  $PI^*$  difference between RCP4.5WA and RCP4.5, averaged over the period 2056–65, due to atmospheric temperature changes in (a) the lower troposphere (1000–350-hPa levels), (b) the upper troposphere (300-, 250-, and 200-hPa levels), (c) the tropopause transition layer (150- and 100-hPa levels) and (d) the lower stratosphere (70-, 50- and 30-hPa levels). (e) The sum of (a) and (b); (f) the sum of (a)–(d).

intensity being caused—in part, perhaps—by the observed cooling of the tropical lower stratosphere (Randel et al. 2009). Apart from two interruptions associated with the eruptions of El Chichón and Pinatubo, that cooling is believed to be largely associated with ozone loss in the lower stratosphere (Thompson and Solomon 2009; Polvani and Solomon 2012), itself driven—perhaps<sup>2</sup>—by an acceleration of the shallow branch of the Brewer–Dobson circulation (BDC).

<sup>2</sup> The ultimate cause and the precise mechanism for the recent cooling of the lower stratosphere remain unclear. Climate models (e.g., Garcia and Randel 2008) clearly suggest that increasing greenhouse gas levels cause an acceleration of the Brewer–Dobson circulation, which, in addition to lowering the concentration of ozone in the lower stratosphere, would contribute to cooling in that region via simple adiabatic upwelling. However, the quantitative increase in greenhouse gas concentrations over the last 30 years may not have been of sufficient amplitude to allow such a forced BDC signal to stand out from the large natural variability, and observational studies of the BDC using different methods do not show a consistent, robust trend in recent decades. See Arblaster et al. (2014) for an up-to-date discussion.

Whether this ozone loss is indeed implicated in the recent increases in tropical cyclone potential intensity is difficult to ascertain from observations alone, as the record is relatively short (35 years) and the ozone’s impacts on  $PI^*$ —if present at all—would be easily overwhelmed by the large natural variability (e.g., ENSO and the quasi-biennial oscillation). Thus, the World Avoided offers an ideal test case, as ozone losses in that scenario are much larger than anything that has been observed in recent decades (i.e., its signal-to-noise ratio is much larger than for the recent past). Notwithstanding that fact, our experiments with WACCM indicate that even huge ozone losses are unable to affect tropical cyclone  $PI^*$ , as the outflow temperatures are largely insensitive to ambient trends in the tropopause layer and the lower stratosphere. While our results will need to be confirmed by future studies with other models, they do point to a rather limited role for ozone depletion (and the projected ozone recovery) in controlling the intensity of tropical cyclones.

*Acknowledgments.* The authors are most grateful to Kerry Emanuel for showing keen interest in their work, for many useful suggestions, and for his kind help in

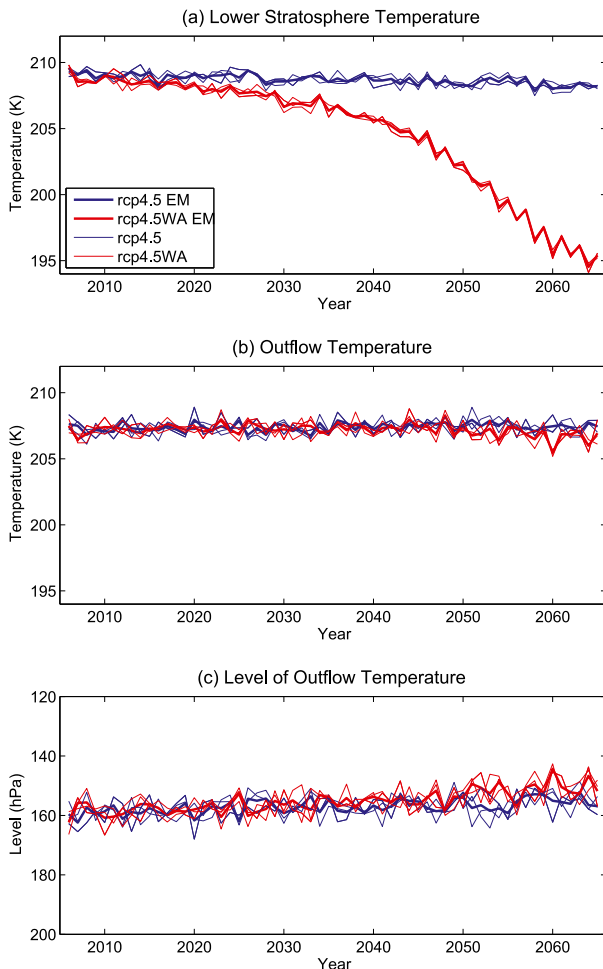


FIG. 11. Annual mean, tropical ( $30^{\circ}\text{S}$  to  $30^{\circ}\text{N}$ ) (a) temperature  $T$  in the lower stratosphere (70-, 50-, and 30-hPa levels), (b) outflow temperature  $T_o$ , and (c) the pressure level of the outflow. Blue curves denote RCP4.5; red curves denote RCP4.5WA. For each scenario, the thick curves show the ensemble mean of the three individual runs (thin curves).

detecting a small bug in the computation of PI in earlier drafts of the paper. They also thank Allison Wing for sharing her results prior to publication. LMP is especially grateful to Michael Mills for help in setting up the World Avoided integrations with WACCM and to Haibo Liu for downloading and preprocessing the CMIP5 data used in this study. The work of LMP is supported, in part, by a grant from the U.S. National Science Foundation to Columbia University. SJC acknowledges support from NSF Grant AGS 1143959 and NOAA Grant NA110AR4310093. We acknowledge high-performance computing support from Yellowstone (ark:/85065/d7wd3xhc) provided by NCAR's Computational and Information Systems Laboratory, sponsored by the National Science Foundation. We

also acknowledge the World Climate Research Programme's Working Group on Coupled Modelling, which is responsible for CMIP, and we thank the climate modeling groups for producing and making available their model output.

## APPENDIX

### CMIP5 Models Used in this Study

The following CMIP5 models were used in this study: ACCESS1.0 (1, 1, 1), ACCESS1.3 (1, 1, 1), BCC\_CSM1.1 (3, 1, 1), CanESM2 (5, 5, 5), CCSM4 (6, 6, 6), CNRM-CM5 (10, 1, 5), CSIRO Mk3.6.0 (10, 5, 10), FGOALS-g2 (5, 1, 1), FIO-ESM (3, 3, 3), GFDL CM3 (5, 1, 1), GFDL-ESM2M (1, 1, 1), GISS-E2-R (5, 5, 1), HadGEM2-CC (1, 1, 1), HadGEM2-ES (4, 1, 4), INM-CM4.0 (1, 1, 1), IPSL-CM5A-LR (5, 4, 4), IPSL-CM5B-LR (1, 1, 1), IPSL-CM5A-MR (1, 1, 1), MIROC5 (4, 1, 3), MIROC-ESM (3, 1, 1), MIROC-ESM-CHEM (1, 1, 1), MPI-ESM-LR (3, 3, 3), MPI-ESM-MR (3, 3, 1), MRI-CGCM3 (3, 1, 1), NorESM1-M (3, 1, 1). The three numbers in parentheses following each model name indicate the size of the ensemble used for the historical, RCP4.5, and RCP8.5 runs, respectively. The multimodel mean is constructed using the ensemble mean of each model.

## REFERENCES

- Arblaster, J., and Coauthors, 2014: Stratospheric ozone changes and climate. Scientific assessment of ozone depletion: 2014, Global Ozone Research and Monitoring Project Rep. 50, 4.1–4.57. [Available online at <http://www.esrl.noaa.gov/csd/assessments/ozone/2014/chapters/2014OzoneAssessment.pdf>.]
- Bister, M., and K. A. Emanuel, 1998: Dissipative heating and hurricane intensity. *Meteor. Atmos. Phys.*, **65**, 233–240, doi:10.1007/BF01030791.
- , and —, 2002: Low frequency variability of tropical cyclone potential intensity: 1. Interannual to interdecadal variability. *J. Geophys. Res.*, **107**, 4801, doi:10.1029/2001JD000776.
- Camargo, S. J., 2013: Global and regional aspects of tropical cyclone activity in the CMIP5 models. *J. Climate*, **26**, 9880–9902, doi:10.1175/JCLI-D-12-00549.1.
- , K. A. Emanuel, and A. H. Sobel, 2007: Use of a genesis potential index to diagnose ENSO effects on tropical cyclone genesis. *J. Climate*, **20**, 4819–4834, doi:10.1175/JCLI4282.1.
- , M. Ting, and Y. Kushnir, 2013: Influence of local and remote SST on North Atlantic tropical cyclone potential intensity. *Climate Dyn.*, **40**, 1515–1529, doi:10.1007/s00382-012-1536-4.
- Emanuel, K. A., 1988: The maximum intensity of hurricanes. *J. Atmos. Sci.*, **45**, 1143–1155, doi:10.1175/1520-0469(1988)045<1143:TMIOH>2.0.CO;2.

- , 1995: Sensitivity of tropical cyclones to surface exchange coefficients and a revised steady-state model incorporating eye dynamics. *J. Atmos. Sci.*, **52**, 3969–3976, doi:10.1175/1520-0469(1995)052<3969:SOTCTS>2.0.CO;2.
- , 2010: Tropical cyclone activity downscaled from NOAA-CIRES reanalysis, 1908–1958. *J. Adv. Model. Earth Syst.*, **2**, 1, doi:10.3894/JAMES.2010.2.1.
- , S. Solomon, D. D. Folini, S. Davis, and C. Cagnazzo, 2013: Influence of tropical tropopause layer cooling on Atlantic hurricane activity. *J. Climate*, **26**, 2288–2301, doi:10.1175/JCLI-D-12-00242.1.
- Farman, J. C., B. G. Gardiner, and J. D. Shanklin, 1985: Large losses of total ozone in Antarctica reveal seasonal ClO<sub>x</sub>/NO<sub>x</sub> interaction. *Nature*, **315**, 207–210, doi:10.1038/315207a0.
- Fueglistaler, S., A. E. Dessler, T. J. Dunkerton, I. Folkins, Q. Fu, and P. W. Mote, 2009: Tropical tropopause layer. *Rev. Geophys.*, **47**, RG1004, doi:10.1029/2008RG000267.
- Garcia, R. R., and W. J. Randel, 2008: Acceleration of the Brewer–Dobson circulation due to increases in greenhouse gases. *J. Atmos. Sci.*, **65**, 2731–2739, doi:10.1175/2008JAS2712.1.
- , D. E. Kinnison, and D. R. Marsh, 2012: “World avoided” simulations with the Whole Atmosphere Community Climate Model. *J. Geophys. Res.*, **117**, D23303, doi:10.1029/2012JD018430.
- Gent, P. R., and Coauthors, 2011: The Community Climate System Model version 4. *J. Climate*, **24**, 4973–4991, doi:10.1175/2011JCLI4083.1.
- Hurrell, J. W., and Coauthors, 2013: The Community Earth System Model: A framework for collaborative research. *Bull. Amer. Meteor. Soc.*, **94**, 1339–1360, doi:10.1175/BAMS-D-12-00121.1.
- Knutson, T. R., and Coauthors, 2010: Tropical cyclones and climate change. *Nat. Geosci.*, **3**, 157–163, doi:10.1038/ngeo779.
- Kossin, J. P., and S. J. Camargo, 2009: Hurricane track variability and secular potential intensity trends. *Climatic Change*, **97**, 329–337, doi:10.1007/s10584-009-9748-2.
- Marsh, D. R., M. J. Mills, D. E. Kinnison, J.-F. Lamarque, N. Calvo, and L. M. Polvani, 2013: Climate change from 1850 to 2005 simulated in CESM1 (WACCM). *J. Climate*, **26**, 7372–7391, doi:10.1175/JCLI-D-12-00558.1.
- Meinshausen, M., S. C. B. Raper, and T. M. L. Wigley, 2011a: Emulating coupled atmosphere–ocean and carbon cycle models with a simpler model, MAGICC6—Part 1: Model description and calibration. *Atmos. Chem. Phys.*, **11**, 1417–1456, doi:10.5194/acp-11-1417-2011.
- , and Coauthors, 2011b: The RCP greenhouse gas concentrations and their extensions from 1765 to 2300. *Climatic Change*, **109**, 213–241, doi:10.1007/s10584-011-0156-z.
- Mendelsohn, R., K. A. Emanuel, S. Chonabayashi, and L. Bakkensen, 2012: The impact of climate change on global tropical cyclone damage. *Nat. Climate Change*, **2**, 205–209, doi:10.1038/nclimate1357.
- Morgenstern, O., P. Braesicke, M. M. Hurwitz, F. M. O’Connor, A. C. Bushell, C. E. Johnson, and J. A. Pyle, 2008: The world avoided by the Montreal Protocol. *Geophys. Res. Lett.*, **35**, L16811, doi:10.1029/2008GL034590.
- Newman, P. A., and Coauthors, 2009: What would have happened to the ozone layer if chlorofluorocarbons (CFCs) had not been regulated? *Atmos. Chem. Phys.*, **9**, 2113–2128, doi:10.5194/acp-9-2113-2009.
- Peduzzi, P., B. Chatenoux, H. Dao, A. D. Bono, C. Herold, J. Kossin, F. Mouton, and O. Nordbeck, 2012: Global trends in tropical cyclone risk. *Nat. Climate Change*, **2**, 289–294, doi:10.1038/nclimate1410.
- Polvani, L. M., and S. Solomon, 2012: The signature of ozone depletion on tropical temperature trends, as revealed by their seasonal cycle in model integrations with single forcings. *J. Geophys. Res.*, **117**, D17102, doi:10.1029/2012JD017719.
- Prather, M., P. Midgley, F. S. Rowland, and R. Stolarski, 1996: The ozone layer: The road not taken. *Nature*, **381**, 551–554, doi:10.1038/381551a0.
- Previdi, M., and L. M. Polvani, 2014: Climate system response to stratospheric ozone depletion and recovery. *Quart. J. Roy. Meteor. Soc.*, **140**, 2401–2419, doi:10.1002/qj.2330.
- Ramanathan, V., 1975: Greenhouse effect due to chlorofluorocarbons: Climatic implications. *Science*, **190**, 50–52, doi:10.1126/science.190.4209.50.
- Ramsay, H. A., 2013: The effects of imposed stratospheric cooling on the maximum intensity of tropical cyclones in axisymmetric radiative–convective equilibrium. *J. Climate*, **26**, 9977–9985, doi:10.1175/JCLI-D-13-00195.1.
- Randel, W. J., and Coauthors, 2009: An update of observed stratospheric temperature trends. *J. Geophys. Res.*, **114**, D02107, doi:10.1029/2008JD010421.
- Shine, K. P., and Coauthors, 2003: A comparison of model-simulated trends in stratospheric temperatures. *Quart. J. Roy. Meteor. Soc.*, **129**, 1565–1588, doi:10.1256/qj.02.186.
- Solomon, S., 1999: Stratospheric ozone depletion: A review of concepts and history. *Rev. Geophys.*, **37**, 275–316, doi:10.1029/1999RG900008.
- Taylor, K. E., R. J. Stouffer, and G. A. Meehl, 2012: An overview of CMIP5 and the experiment design. *Bull. Amer. Meteor. Soc.*, **93**, 485–498, doi:10.1175/BAMS-D-11-00094.1.
- Thompson, D. W. J., and S. Solomon, 2009: Understanding recent stratospheric climate change. *J. Climate*, **22**, 1934–1943, doi:10.1175/2008JCLI2482.1.
- , —, P. J. Kushner, M. H. England, K. M. Grise, and D. Karoly, 2011: Signatures of the Antarctic ozone hole in Southern Hemisphere surface climate change. *Nat. Geosci.*, **4**, 741–749, doi:10.1038/ngeo1296.
- Ting, M., S. J. Camargo, C. Li, and Y. Kushnir, 2015: Natural and forced North Atlantic hurricane potential intensity change in CMIP5 models. *J. Climate*, **28**, 3926–3942, doi:10.1175/JCLI-D-14-00520.1.
- Uppala, S. M., and Coauthors, 2005: The ERA-40 Re-Analysis. *Quart. J. Roy. Meteor. Soc.*, **131**, 2961–3012, doi:10.1256/qj.04.176.
- Van Vuuren, D. P., and Coauthors, 2011: The representative concentration pathways: An overview. *Climatic Change*, **109**, 5–31, doi:10.1007/s10584-011-0148-z.
- Vecchi, G. A., and B. J. Soden, 2007: Effect of remote sea surface temperature change on tropical cyclone potential intensity. *Nature*, **450**, 1066–1070, doi:10.1038/nature06423.
- , S. Fueglistaler, I. M. Held, T. R. Knutson, and M. Zhao, 2013: Impacts of atmospheric temperature trends on tropical cyclone activity. *J. Climate*, **26**, 3877–3891, doi:10.1175/JCLI-D-12-00503.1.
- Velders, G. J., S. O. Andersen, J. S. Daniel, D. W. Fahey, and M. McFarland, 2007: The importance of the Montreal Protocol in protecting climate. *Proc. Natl. Acad. Sci. USA*, **104**, 4814–4819, doi:10.1073/pnas.0610328104.
- Wang, S., S. J. Camargo, A. H. Sobel, and L. M. Polvani, 2014: Impact of the tropopause temperature on the intensity of

- tropical cyclones: An idealized study using a mesoscale model. *J. Atmos. Sci.*, **71**, 4333–4348, doi:[10.1175/JAS-D-14-0029.1](https://doi.org/10.1175/JAS-D-14-0029.1).
- Wing, A. A., A. H. Sobel, and S. J. Camargo, 2007: Relationship between the potential and actual intensities of tropical cyclones on interannual time scales. *Geophys. Res. Lett.*, **34**, L08810, doi:[10.1029/2006GL028581](https://doi.org/10.1029/2006GL028581).
- , K. Emanuel, and S. Solomon, 2015: On the factors affecting trends and variability in tropical cyclone potential intensity. *Geophys. Res. Lett.*, **42**, 8669–8677, doi:[10.1002/2015GL066145](https://doi.org/10.1002/2015GL066145).
- World Meteorological Organization, 2007: Scientific assessment of ozone depletion: 2006. Global Ozone Research and Monitoring Project Rep. 50, 572 pp.
- Wu, Y., L. M. Polvani, and R. Seager, 2013: The importance of the Montreal Protocol in protecting Earth's hydroclimate. *J. Climate*, **26**, 4049–4068, doi:[10.1175/JCLI-D-12-00675.1](https://doi.org/10.1175/JCLI-D-12-00675.1).